

# Multi-resolution polymer Brownian dynamics with hydrodynamic interactions

Edward Rolls, and Radek Erban

Citation: [The Journal of Chemical Physics](#) **148**, 194111 (2018); doi: 10.1063/1.5018595

View online: <https://doi.org/10.1063/1.5018595>

View Table of Contents: <http://aip.scitation.org/toc/jcp/148/19>

Published by the [American Institute of Physics](#)

---

## Articles you may be interested in

[Brownian dynamics with hydrodynamic interactions](#)

The Journal of Chemical Physics **69**, 1352 (1978); 10.1063/1.436761

[An iterative method for hydrodynamic interactions in Brownian dynamics simulations of polymer dynamics](#)

The Journal of Chemical Physics **147**, 024904 (2017); 10.1063/1.4993218

[Communication: Adaptive boundaries in multiscale simulations](#)

The Journal of Chemical Physics **148**, 141104 (2018); 10.1063/1.5025826

[Efficient Brownian Dynamics of rigid colloids in linear flow fields based on the grand mobility matrix](#)

The Journal of Chemical Physics **148**, 194112 (2018); 10.1063/1.5027063

[MSM/RD: Coupling Markov state models of molecular kinetics with reaction-diffusion simulations](#)

The Journal of Chemical Physics **148**, 214107 (2018); 10.1063/1.5020294

[Communication: Diffusion constant in supercooled water as the Widom line is crossed in no man's land](#)

The Journal of Chemical Physics **148**, 191102 (2018); 10.1063/1.5029822

---

PHYSICS TODAY

WHITEPAPERS

### ADVANCED LIGHT CURE ADHESIVES

Take a closer look at what these environmentally friendly adhesive systems can do

READ NOW

PRESENTED BY  
**MASTERBOND**  
ADHESIVES | SEALANTS | COATINGS

# Multi-resolution polymer Brownian dynamics with hydrodynamic interactions

Edward Rolls<sup>a)</sup> and Radek Erban<sup>b)</sup>

Mathematical Institute, University of Oxford, Radcliffe Observatory Quarter, Woodstock Road, Oxford OX2 6GG, United Kingdom

(Received 7 December 2017; accepted 30 April 2018; published online 18 May 2018)

A polymer model given in terms of beads, interacting through Hookean springs and hydrodynamic forces, is studied. A Brownian dynamics description of this bead-spring polymer model is extended to multiple resolutions. Using this multiscale approach, a modeller can efficiently look at different regions of the polymer in different spatial and temporal resolutions with scalings given for the number of beads, statistical segment length, and bead radius in order to maintain macro-scale properties of the polymer filament. The Boltzmann distribution of a Gaussian chain for differing statistical segment lengths gives a diffusive displacement equation for the multi-resolution model with a mobility tensor for different bead sizes. Using the pre-averaging approximation, the translational diffusion coefficient is obtained as a function of the inverse of a matrix and then in closed form in the long-chain limit. This is then confirmed with numerical experiments. © 2018 Author(s). All article content, except where otherwise noted, is licensed under a Creative Commons Attribution (CC BY) license (<http://creativecommons.org/licenses/by/4.0/>). <https://doi.org/10.1063/1.5018595>

## I. INTRODUCTION

There have been many studies which use a Brownian dynamics (BD) model for polymers with hydrodynamic interactions as a method to coarse-grain complex interactions at the atomic level to study macromolecules in biology and materials science, for example, stepping kinetics of kinesin<sup>1</sup> and dynamics for  $\lambda$ -phage DNA<sup>2–4</sup> and for polystyrene.<sup>5,6</sup> BD models can be written in terms of stochastic equations for the time evolution of a system, which are valid where some entities of the system (in this case, beads on a chain) act on both temporal and spatial scales significantly different to the underlying solvent. In this work, we use a BD model to describe a polymer as a collection of beads connected by Hookean springs.<sup>7</sup> We extend the BD modeling framework to allow a polymer molecule to be considered on multiple resolutions so that the statistical segment length and bead size vary along the polymer as well as the time step used for simulating BD; i.e., we consider multiple resolutions of both spatial and temporal scales for the polymer.

The use of a multi-resolution model allows us to look at areas of interest on the polymer in additional detail while modeling less important areas in less detail and maintaining global properties of the polymer. The main benefit of this form of hybrid modeling is in computational savings compared to modeling the entire domain in high resolution and has become an increasingly popular technique in recent years as a method to look at complex models on larger spatial scales with more biologically relevant time scales.<sup>8–11</sup> This is useful, for

example, in modeling the interaction between a DNA-binding protein and a DNA filament, where only the area near the protein needs to be modelled in a high resolution and other areas can be modelled in a lower resolution. A similar approach to the one taken in this paper has been considered in our previous work in the case where hydrodynamic interactions can be neglected.<sup>12</sup>

This work acts as an extension to analytic results for properties of the single-scale polymer dynamical simulations with hydrodynamic interactions. Much of the initial analysis of the single-scale model was done by Kirkwood and Riseman,<sup>13</sup> who introduced elements of the BD model and gave an approximation to the translational diffusion coefficient which uses equilibrium averages for internal configurations. Following this, Zimm<sup>14</sup> found an approximation to the translational diffusion coefficient by pre-averaging (PA) the inter-particle distances in the hydrodynamic interaction tensor. Öttinger<sup>15</sup> found a more accurate approximation equivalent to the previous work of Fixman<sup>16</sup> by considering the centre of hydrodynamic resistance and manipulating the diffusive displacement equation, which is the work we will build on to obtain equations for the diffusion coefficient, partly because its formulation has a natural extension to multi-resolution modeling.

In this paper, we start by formulating the model using a statistical physics description and using the Boltzmann distribution to form a mechanical model, similar to how the single-scale model is built by Doi and Edwards.<sup>7</sup> We also define the mobility matrix, which comes from extending the Rotne-Prager-Yamakawa tensor<sup>17,18</sup> to allow for different bead sizes by considering fluid dynamics properties.<sup>19</sup> This provides a diffusive displacement equation for the new model, as well as formulations for the distribution of inter-bead distances,

<sup>a)</sup>Electronic mail: [edward.rolls@pmb.ox.ac.uk](mailto:edward.rolls@pmb.ox.ac.uk)

<sup>b)</sup>Electronic mail: [erban@maths.ox.ac.uk](mailto:erban@maths.ox.ac.uk). URL: <http://people.maths.ox.ac.uk/erban/>.

including the root mean squared (rms) end-to-end distance. From this description, we form two approximations for the translational diffusion coefficient: one as a solution to a matrix inversion problem and another in closed form in the long-chain limit. This form of the diffusion is used to give us scaling laws for the statistical segment length, the bead radius, and the number of beads in each region of the polymer. These scaling laws maintain the global properties of the rms end-to-end distance and diffusion.

A number of algorithms have been proposed for efficient BD simulations with hydrodynamic interactions for the single-scale polymer model in the literature.<sup>20–23</sup> In Sec. IV, we adapt the Ermak-McCammon algorithm<sup>24</sup> by varying the time step along the polymer in order for BD simulations of the displacement equation to take place. We conclude with illustrative computational results confirming the presented theory in Sec. V.

## II. MULTI-RESOLUTION BEAD-SPRING MODEL

As a model for a polymer, we use an extension to the bead-spring model which has existed for over 60 years.<sup>7,25,26</sup> This method of modeling has  $N$  beads connected with  $(N - 1)$  Hookean springs, neither of which seek to have physical significance as such, but represent a coarse-grained description of the direction the polymer is coiled. Our multi-resolution extension allows different beads to have different sizes and the statistical segment length between the adjacent beads to vary.

To form the multi-resolution model, we start with a static description of the chain as an extension of the Gaussian chain model, where much of the analysis follows from the treatment given by Doi and Edwards,<sup>7</sup> but with varying bond lengths. We use this to derive a potential for spring constants using the Boltzmann distribution which in turn is used to form the dynamic model with hydrodynamic interactions given from a multi-resolution extension of the Rotne-Prager-Yamakawa tensor.<sup>17–19</sup> The process of obtaining a coarse-grained model for a polymer from its microscopic description has been discussed by Underhill and Doyle.<sup>27</sup>

### A. Static description

We consider a bead-spring polymer model with  $N$  beads, where the positions of the beads of the chain are given by  $\mathbf{r}_n$  so that  $\mathbf{R}_n = \mathbf{r}_{n+1} - \mathbf{r}_n$ , for  $n = 1, 2, \dots, N - 1$ , are the corresponding bond vectors. In the multi-resolution bead-spring model, the distribution  $\psi_n$  for the  $n$ th bond vector  $\mathbf{R}_n$ ,  $n = 1, 2, \dots, N - 1$ , can vary along the chain

$$\psi_n(\mathbf{R}_n) = \left( \frac{3}{2\pi b_n^2} \right)^{3/2} \exp\left(-\frac{3\mathbf{R}_n^2}{2b_n^2}\right), \quad (1)$$

where the statistical segment lengths  $\langle \mathbf{R}_n^2 \rangle = b_n^2$  are allowed to vary along the filament. In the special case  $b = b_n$ , for all  $n = 1, 2, \dots, N - 1$ , Eq. (1) reduces to the standard Gaussian chain model.<sup>7</sup> Using (1), the distribution of  $\mathbf{r}_{mn} = \mathbf{r}_n - \mathbf{r}_m$ , for  $n \neq m$ , is given by

$$\Phi(\mathbf{r}_{mn}) = \left( \frac{3}{2\pi\mu_{mn}^2} \right)^{3/2} \exp\left(-\frac{3(\mathbf{r}_n - \mathbf{r}_m)^2}{2\mu_{mn}^2}\right), \quad (2)$$

where we define

$$\mu_{mn}^2 = \sum_{k=\min\{m,n\}}^{\max\{m,n\}-1} b_k^2.$$

If we define the rms end-to-end distance  $\mu = \langle \mathbf{R}^2 \rangle^{1/2}$ , where  $\mathbf{R}$  is the vector from the first to the last bead, then we find

$$\mu = \sqrt{\langle (\mathbf{r}_N - \mathbf{r}_1)^2 \rangle} = \mu_{1N} = \sqrt{\sum_{k=1}^{N-1} b_k^2}. \quad (3)$$

Using (1), the conformational distribution function of the chain is given by

$$\begin{aligned} \Psi(\{\mathbf{r}_n\}) &= \prod_{n=1}^{N-1} \psi_n(\mathbf{R}_n) \\ &= \left( \frac{3}{2\pi \prod_{n=1}^{N-1} b_n^2} \right)^{3/2} \exp\left(-\sum_{n=1}^{N-1} \frac{3\mathbf{R}_n^2}{2b_n^2}\right). \end{aligned} \quad (4)$$

If we consider a mechanical model of such a polymer chain, this model would have potential energy,

$$U(\{\mathbf{r}_n\}) = \frac{3k_B T}{2} \sum_{n=1}^{N-1} \frac{(\mathbf{r}_{n+1} - \mathbf{r}_n)^2}{b_n^2}, \quad (5)$$

to give an identical Boltzmann distribution to Eq. (4).

### B. Dynamic model description

Using potential (5), we form a diffusive displacement equation for the dynamic model<sup>28</sup> for the  $n$ th bead at time  $t$ ,

$$d\mathbf{r}_n = \left( \sum_{m=1}^N \mathbf{H}_{nm} \frac{\partial U}{\partial \mathbf{r}_m} + \nabla_m \cdot \mathbf{H}_{nm} \right) dt + \sum_{m=1}^N \mathbf{B}_{nm} d\mathbf{W}_m, \quad (6)$$

where  $\mathbf{H}_{mn} \in \mathbb{R}^{3 \times 3}$  is a positive-definite symmetric mobility matrix,  $d\mathbf{W}_m \in \mathbb{R}^3$  is a Wiener process, and we define  $\mathbf{B}_{mn} \in \mathbb{R}^{3 \times 3}$  so that

$$\mathbf{H}_{mn} = \frac{1}{2k_B T} \sum_{k=1}^N \mathbf{B}_{mk} \mathbf{B}_{nk}^T, \quad (7)$$

where  $T$  is the absolute temperature, superscript T (roman font) denotes the transpose of a matrix, and  $k_B$  is the Boltzmann constant. The matrix  $\mathbf{B}_{mk}$  exists due to the positive-definiteness of  $\mathbf{H}_{mn}$  and can be found by performing a decomposition (e.g., the Cholesky decomposition). In choosing the mobility matrix, we would like to vary the bead sizes along the filament, which can be used to ensure that macroscopic properties of the polymer remain constant. Therefore, the bead size  $\sigma_n$  becomes a parameter of the  $n$ th bead.

Rolls *et al.*<sup>12</sup> used the diagonal mobility tensor which works as an extension of the Rouse model

$$\mathbf{H}_{mn} = \begin{cases} \frac{1}{6\pi\eta\sigma_n} \mathbf{I}, & \text{if } m = n, \\ \mathbf{0}, & \text{if } m \neq n, \end{cases} \quad (8)$$

where  $\eta$  is the dynamic viscosity and  $\mathbf{I} \in \mathbb{R}^{3 \times 3}$  is the identity matrix. One of the purposes of this paper is to extend model (8) to include hydrodynamic interactions. Many models which include hydrodynamic interactions where beads are of equal sizes use the Rotne-Prager-Yamakawa<sup>17,18</sup> tensor. This has been extended by Zuk *et al.*<sup>19</sup> to allow for the beads of different sizes. To formulate it, we denote for beads  $m$  and  $n$

$$\begin{aligned} \sigma_{mn} &= |\sigma_n - \sigma_m|, \\ r_{mn} &= |\mathbf{r}_n - \mathbf{r}_m|, \end{aligned}$$

where  $\sigma_m$  (respectively,  $\sigma_n$ ) is the radius of bead  $m$  (respectively,  $n$ ) and  $r_{mn}$  is the distance between beads. We also denote by  $\hat{\mathbf{r}}_{mn}$  the unit vector between beads, i.e.,

$$\hat{\mathbf{r}}_{mn} = \frac{\mathbf{r}_n - \mathbf{r}_m}{r_{mn}}.$$

Then the Rotne-Prager-Yamakawa-type mobility tensor is given by<sup>19</sup>

$$\mathbf{H}_{mn} = \begin{cases} \frac{1}{6\pi\eta\sigma_n} \mathbf{I}, & \text{if } m = n; \\ \frac{1}{8\pi\eta r_{mn}} \left[ \left( 1 + \frac{\sigma_n^2 + \sigma_m^2}{3r_{mn}^2} \right) \mathbf{I} + \left( 1 - \frac{\sigma_n^2 + \sigma_m^2}{r_{mn}^2} \right) \hat{\mathbf{r}}_{mn} \otimes \hat{\mathbf{r}}_{mn} \right], & \text{if } \sigma_n + \sigma_m < r_{mn}; \\ \frac{1}{6\pi\eta\sigma_n\sigma_m} \left[ \frac{16r_{mn}^3(\sigma_n + \sigma_m) - (\sigma_{mn}^2 + 3r_{mn}^2)^2}{32r_{mn}^3} \mathbf{I} + \frac{3(\sigma_{mn}^2 - r_{mn}^2)^2}{32r_{mn}^3} \hat{\mathbf{r}}_{mn} \otimes \hat{\mathbf{r}}_{mn} \right], & \text{if } \sigma_{mn} < r_{mn} \leq \sigma_n + \sigma_m; \\ \frac{1}{6\pi\eta \max\{\sigma_n, \sigma_m\}} \mathbf{I}, & \text{if } r_{mn} \leq \sigma_{mn}; \end{cases} \quad (9)$$

which is positive-definite, symmetric, and continuous for sufficiently small  $\sigma_n$  for all  $n$ . As we are dealing with an unconfined system, this gives  $\nabla_m \cdot \mathbf{H}_{nm} = 0$ , which simplifies the diffusive displacement equation (6) to

$$d\mathbf{r}_n = \left( \sum_{m=1}^N \mathbf{H}_{nm} \mathbf{F}_m \right) dt + \sum_{m=1}^N \mathbf{B}_{nm} d\mathbf{W}_m, \quad (10)$$

where  $\mathbf{B}_{mn} \in \mathbb{R}^{3 \times 3}$  are given by (7) which exists by the positive-definite symmetric property of  $\mathbf{H}_{mn}$  and inter-bead force  $\mathbf{F}_m$  is found by differentiating the potential (5) to get

$$\mathbf{F}_m = \frac{3k_B T}{b_{m-1}^2} (\mathbf{r}_{m-1} - \mathbf{r}_m) + \frac{3k_B T}{b_m^2} (\mathbf{r}_{m+1} - \mathbf{r}_m), \quad (11)$$

for  $m = 2, 3, \dots, N-1$ . We treat the end beads  $\mathbf{r}_1$  and  $\mathbf{r}_N$  by (11) as well, where we consider auxiliary beads  $\mathbf{r}_0$  and  $\mathbf{r}_{N+1}$  defined such that  $\mathbf{r}_0 = \mathbf{r}_1$  and  $\mathbf{r}_N = \mathbf{r}_{N+1}$ .

### III. APPROXIMATION OF THE DIFFUSION COEFFICIENT AND IDEAL PARAMETERISATION

We take a similar approach to that of Öttinger<sup>15</sup> to find an approximation for the diffusion of the multi-resolution model. This is then used in conjunction with knowledge of the distribution of the rms end-to-end vector to inform the scaling for a multiscale simulation so that properties of interest match up to the high-resolution model.

#### A. Diffusion approximation

To find an approximation to the diffusion for the mobility tensor with hydrodynamic terms included, we use the pre-averaging approximation<sup>7</sup> introduced by Zimm.<sup>14</sup> Considering near-equilibrium dynamics, we replace the mobility

tensor  $\mathbf{H}_{mn}$  with its equilibrium average  $\langle \mathbf{H}_{mn} \rangle_{\text{eq}}$ , using  $\Psi$  from Eq. (4),

$$\mathbf{H}_{mn} \rightarrow \langle \mathbf{H}_{mn} \rangle_{\text{eq}} = \int \mathbf{H}_{mn} \Psi(\{\mathbf{r}_n\}) d\{\mathbf{r}_n\}.$$

If we assume that  $\sigma_n + \sigma_{n+1} < b_n$  for all  $n \leq N-1$ , then our equilibrium distribution  $\langle \mathbf{H}_{mn} \rangle_{\text{eq}}$  for off-diagonal entries  $m \neq n$  becomes

$$\begin{aligned} \langle \mathbf{H}_{mn} \rangle_{\text{eq}} &= \frac{1}{8\pi\eta} \left[ \left\langle \frac{1}{r_{mn}} \right\rangle_{\text{eq}} \langle \mathbf{I} + \hat{\mathbf{r}}_{mn} \otimes \hat{\mathbf{r}}_{mn} \rangle_{\text{eq}} \right. \\ &\quad \left. + (\sigma_n^2 + \sigma_m^2) \left\langle \frac{1}{r_{mn}^3} \right\rangle_{\text{eq}} \left\langle \frac{\mathbf{I}}{3} - \hat{\mathbf{r}}_{mn} \otimes \hat{\mathbf{r}}_{mn} \right\rangle_{\text{eq}} \right], \end{aligned}$$

where we have used that the distribution of  $\hat{\mathbf{r}}_{mn}$  is independent of  $r_{mn}$ . Using  $\langle \hat{\mathbf{r}}_{mn} \otimes \hat{\mathbf{r}}_{mn} \rangle_{\text{eq}} = \mathbf{I}/3$ , the second term cancels and we obtain  $\langle \mathbf{H}_{mn} \rangle_{\text{eq}} = \hat{H}_{mn} \mathbf{I}$ , where

$$\hat{H}_{mn} = \begin{cases} \frac{1}{6\pi\eta\sigma_n}, & \text{for } m = n, \\ \frac{1}{6\pi\eta \left\langle \frac{1}{r_{mn}} \right\rangle_{\text{eq}}}, & \text{for } m \neq n. \end{cases}$$

Using (2), we obtain

$$\hat{H}_{mn} = \begin{cases} \frac{1}{6\pi\eta\sigma_n}, & \text{for } m = n, \\ \frac{1}{\mu_{mn} \eta \pi \sqrt{6\pi}}, & \text{for } m \neq n. \end{cases} \quad (12)$$

In the single-scale model, where  $b_n = b$  and  $\sigma_n = \sigma$  for all  $n$ , Eq. (12) generalises to the equation for the pre-averaged tensor in the book by Doi and Edwards.<sup>7,14</sup> Consequently, by pre-averaging Eq. (10), we find

$$d\mathbf{r}_n = \left( \sum_{m=1}^N \widehat{H}_{nm} \mathbf{F}_m \right) dt + \sum_{m=1}^N \widehat{B}_{nm} d\mathbf{W}_m, \quad (13)$$

where

$$\widehat{H}_{mn} = \frac{1}{2k_B T} \sum_{k=1}^N \widehat{B}_{mk} \widehat{B}_{nk}. \quad (14)$$

Following Öttinger,<sup>28</sup> we define the hydrodynamic center of resistance  $\mathbf{r}_h$  by

$$\mathbf{r}_h = \sum_{n=1}^N l_n \mathbf{r}_n, \quad \text{where} \quad l_n = \frac{\sum_{m=1}^N \widehat{H}_{nm}^{-1}}{\sum_{m,k=1}^N \widehat{H}_{km}^{-1}}.$$

Multiplying Eq. (13) by  $l_n$  and summing over all  $n$ , we get

$$d\mathbf{r}_h = \left( \sum_{m,n=1}^N l_n \widehat{H}_{nm} \mathbf{F}_m \right) dt + \sum_{m=1}^N \left( \sum_{n=1}^N l_n \widehat{B}_{nm} \right) d\mathbf{W}_m.$$

Using (11), the first term on the right-hand side is zero and the second term is a linear combination of Wiener processes, which itself is a Wiener process with the translational diffusion coefficient

$$D_h = \frac{1}{2} \sum_{m=1}^N \left( \sum_{n=1}^N l_n \widehat{B}_{nm} \right)^2.$$

Using (14) and the definition of  $l_n$ , we obtain

$$D_h = k_B T \left( \sum_{m,n=1}^N \widehat{H}_{mn}^{-1} \right)^{-1}. \quad (15)$$

This forms a matrix equation to provide the pre-averaged approximation for the translational diffusion coefficient.

Our analysis in this section used a general multi-resolution model consisting of  $N$  beads with sizes  $\sigma_n$ ,  $n = 1, 2, \dots, N$ , connected by  $N - 1$  springs with statistical segment lengths  $b_n$ ,  $n = 1, 2, \dots, N - 1$ . In applications to multiscale computations, we are mostly interested in chains which are split into  $M$  regions (where  $M \ll N$ ) of constant statistical segment length. In the remainder of this paper and the Appendix, we shall use lower case Greek subscripts  $\alpha$  (respectively,  $\beta$  and  $\gamma$ ) to denote regions, while  $n$  (respectively,  $m$  and  $k$ ) are indices referring to the numbers of individual beads and springs along the polymer chain.

By generalizing the approach of Öttinger<sup>28</sup> and Fixman,<sup>16</sup> we can form a first-order approximation of this matrix equation in the long-chain limit as the number of beads  $N \rightarrow \infty$ , which gives the diffusion constant

$$D_h = \frac{\Gamma^2(1/4)}{4\pi^2 \sqrt{3}} \frac{k_B T}{\eta \mu} \approx 0.1922 \frac{k_B T}{\eta \mu}. \quad (16)$$

The derivation for this approximation is in the Appendix. There are also other formulations of the diffusion constant in the long-chain limit for the single-scale model; for example, the Kirkwood-Riseman formulation<sup>13,29</sup> has the constant 0.1955 in front of the expression in Eq. (16).

## B. Scaling of parameters

As a bead-spring model is used to give a coarse-grained representation of a filament, statistical segment length and bead radius are not physical quantities, so we allow these

parameters of the model to vary in order to achieve desired statistics of interest for the polymer. In our previous work,<sup>12</sup> the whole-system statistics of interest have been the rms end-to-end distance  $\mu$  and translational diffusion coefficient  $D_h$  of a polymer chain. In this paper, we will consider three quantities which multi-resolution simulations should preserve: the rms end-to-end distance  $\mu$ , diffusion coefficient  $D_h$ , and the strength of hydrodynamic interactions<sup>30</sup> defined in terms of the parameter  $h^*$  by

$$h^* = \sqrt{\frac{3}{\pi}} \frac{\sigma}{b},$$

where  $b$  is the statistical segment length and  $\sigma$  is the bead radius. From a theoretical standpoint, a value for  $h^* \approx 0.25$  minimises the effect of chain length.<sup>31</sup> Similar values can also match experimental results for viscoelastic properties; for example, the Flory-Fox parameter can match experimental values<sup>30</sup> for  $h^* \approx 0.267$ . In the multi-resolution model, in order to maintain a consistent value for the strength of hydrodynamic interactions, we therefore scale parameters in order to keep  $h^*$  constant throughout simulations.

The multi-resolution polymer simulations will be compared to the highest resolution model, which will be the single-scale model of the polymer in the maximum detail required. In single-scale models, we can modify the whole-system statistics by varying the statistical segment length  $b$ , the bead radius  $\sigma$ , and the total number of beads  $N$ . In single-scale models, we need to select a level of detail for the entire chain as an additional constraint, but by modeling on multiple scales, we instead get to select the resolution of different regions of the polymer so that only regions of particular interest need to be in the highest level of detail. To parameterize the highest resolution model, we select  $b$  to give the desired value for the rms end-to-end distance  $\mu$ , from Eq. (3), i.e.,  $b = \mu(N - 1)^{-1/2}$ . Selecting a value for  $\sigma$  is a bit more subtle than for models without hydrodynamic interactions,<sup>12</sup> as the inclusion of the hydrodynamic interactions mean the leading order long chain diffusion approximation in Eq. (16) is independent of  $\sigma$ ; i.e., we cannot use  $D_h$ . We use the strength of hydrodynamic interaction  $h^*$  to select an appropriate value of  $\sigma$ . For all simulations in this paper, we use  $\sigma = b/4$ .

Once we have defined the highest resolution model, with statistical segment length  $b$ , bead radius  $\sigma$ , and total beads  $N$ , we can seek to define the scalings for the multi-resolution model, where different regions coarse grain the original model to differing extents. This multi-resolution model should be seen as a reduction in the degrees of freedom of the highest resolution model, which itself is a coarse-grained description of physical reality. We divide the highest-resolution polymer into  $M$  regions each containing  $\widetilde{N}_\alpha$  springs for  $\alpha = 1, 2, \dots, M$  such that  $\sum_{\alpha=1}^M \widetilde{N}_\alpha = N - 1$ . Each region of the multi-resolution model has an associated (integer-valued) resolution  $s_\alpha$  such that  $s_\alpha^2 \mid \widetilde{N}_\alpha$ , where we use the divisibility symbol  $a \mid b$  if there exists an integer  $n$  such that  $an = b$  and the symbol  $a \nmid b$  where no such integer  $n$  exists. Larger values of  $s_\alpha$  represent coarser regions, and  $s_\alpha = 1$  gives the highest resolution model. In the  $\alpha$ th region of the multi-resolution model, we



have  $N_\alpha$  springs with statistical segment length  $b_\alpha$  given by

$$N_\alpha = \frac{\tilde{N}_\alpha}{s_\alpha^2}, \quad b_\alpha = s_\alpha b, \quad \sigma_\alpha = s_\alpha \sigma, \quad (17)$$

where the definition of the bead radius,  $\sigma_\alpha$ , is slightly modified for the boundary beads; scalings (17) apply to beads where both adjacent springs have the same statistical segment length  $b_\alpha$ . On the boundaries between regions  $\alpha$  and  $\alpha + 1$ , for  $\alpha = 1, 2, \dots, M - 1$ , we take the bead radius to be  $((\sigma_\alpha^2 + \sigma_{\alpha+1}^2)/2)^{1/2}$ , and for end beads at the start and end of the polymer, we take  $\sigma_1/\sqrt{2}$  and  $\sigma_M/\sqrt{2}$ , respectively. By applying scalings (17), Eq. (3) gives the expected rms end-to-end distance for the filament at equilibrium to be  $\mu = b(N - 1)^{1/2}$ ; i.e., it is equal to the highest resolution model. The translational diffusion coefficient for the polymer in the long-chain limit, Eq. (16), is also invariant to the number of regions, as well as the size and resolution of each region, and the strength of hydrodynamic interactions is constant along the filament.

#### IV. SIMULATION METHOD

We solve the diffusive displacement equation for the polymer (10) by using a modified version of the Ermak-McCammon algorithm,<sup>24</sup> for which different regions have different time step sizes. The key idea for the modified algorithm is to keep track of the behavior of beads modelled with a higher resolution (and with smaller time steps) to give an average of the hydrodynamic forces exerted on the coarsely modelled beads between the larger time steps on which they are modelled.

If the highest resolution model uses time step  $\Delta t$ , then with the notation of Sec. III B, we define the time step associated with the  $\alpha$ th region as

$$\Delta t_\alpha = s_\alpha^3 \Delta t,$$

where  $s_\alpha$  is the (integer-valued) resolution of the  $\alpha$ th region,  $\alpha = 1, 2, \dots, M$ . When setting up the system, the resolution for any two regions  $\alpha$  and  $\beta$  must be such that either  $s_\alpha^3 |s_\beta^3$  or  $s_\beta^3 |s_\alpha^3$  to ensure the time steps of the coarser regions are multiples of those for the finer regions. We choose this scaling to ensure numerical stability of simulations so that the size of the tension term for a bead is much smaller than the statistical segment length with adjacent beads. In the case of a bead lying between two regions, we take the time step to be the minimum value of the time steps given by each region.

The highest resolution model updates time at integer multiples of  $\Delta t$ , i.e., we compute the polymer state at times  $t = i\Delta t$ , where  $i = 0, 1, 2, 3, \dots$ . Considering the multi-resolution model, we can formally write the update rule (from time  $i\Delta t$  to time  $(i + 1)\Delta t$ ) for the  $n$ th bead, for  $n = 1, 2, \dots, N$ , in region  $\alpha_n$  as

$$\mathbf{r}_n((i + 1)\Delta t) = \mathbf{r}_n(i\Delta t) + Q(s_{\alpha_n}^3, i + 1) \left( \tilde{\boldsymbol{\rho}}_n(i\Delta t) + \sum_{m=1}^N Q(s_{\alpha_m}^3, i + 1) \mathbf{H}_{nm} \tilde{\mathbf{F}}_{mn}(i\Delta t) \right), \quad (18)$$

where  $\mathbf{H}_{nm}$  is the mobility tensor given in Eq. (9),  $\tilde{\mathbf{F}}_{mn}$  and  $\tilde{\boldsymbol{\rho}}_n$  are the discretized force and noise terms given below, and the

function  $Q$  is defined for integers  $i$  and  $j$  by

$$Q(j, i) = \begin{cases} 1, & \text{if } j | i, \\ 0, & \text{if } j \nmid i. \end{cases}$$

To define discretized force and noise terms, we denote by  $\alpha_n$  (respectively,  $\beta_n$ ) the resolution region for the  $n$ th bead (respectively, spring). Note that for beads with both adjacent springs in the same region, we will see  $\alpha_n = \beta_n$ ; however, between regions, a bead takes the smaller time step of the adjacent regions, so we may see  $\alpha_n \neq \beta_n$ . In the update rule (18), the time step is incorporated in the force term. We define the force multiplied by the time step for the  $m$ th bead by

$$\begin{aligned} \tilde{\mathbf{F}}_m(i\Delta t) &= \frac{3k_B T}{b_{m-1}^2} (\mathbf{r}_{m-1}(i\Delta t) - \mathbf{r}_m(i\Delta t)) \Delta t_{\beta_{m-1}} \\ &\quad + \frac{3k_B T}{b_m^2} (\mathbf{r}_{m+1}(i\Delta t) - \mathbf{r}_m(i\Delta t)) \Delta t_{\beta_m}. \end{aligned}$$

This force term is used as a part of a tension term which includes a memory component for larger time steps, as explained in Table I,

$$\tilde{\mathbf{F}}_{mn}(i\Delta t) = \begin{cases} \tilde{\mathbf{F}}_m(i\Delta t), & \text{if } s_{\alpha_n} < s_{\alpha_m}, \\ \sum_{p=0}^{(s_{\alpha_n}/s_{\alpha_m})^3 - 1} \tilde{\mathbf{F}}_m((i - p)\Delta t), & \text{otherwise.} \end{cases}$$

The random displacement term  $\tilde{\boldsymbol{\rho}}_n$  has a multivariate Gaussian distribution defined by the moments

$$\begin{aligned} \langle \tilde{\boldsymbol{\rho}}_n \rangle &= 0, \\ \langle \tilde{\boldsymbol{\rho}}_m \otimes \tilde{\boldsymbol{\rho}}_n \rangle &= 2k_B T \mathbf{H}_{mn} \max(\Delta t_{\alpha_m}, \Delta t_{\alpha_n}), \end{aligned}$$

where we use the maximum as this term is only expressed on the larger of the two time steps associated with the beads, as laid out below. To calculate the  $\tilde{\boldsymbol{\rho}}_n$  terms, we use an adapted version of the Ermak-McCammon algorithm<sup>24</sup> so that when we flatten the tensor  $\mathbf{H}_{mn}$  into a matrix  $\mathbf{H}$ , we do so by re-ordering the beads so that beads with smaller time steps have a smaller index than beads with larger time steps. Having made this adjustment, we can reduce the computational load of the Cholesky decomposition done by the Ermak-McCammon algorithm (an  $\mathcal{O}(N^3)$  calculation<sup>32</sup>) by only calculating the submatrix made up of the rows and columns of the matrix corresponding to beads which are being calculated on that particular time step. Therefore, if there are  $N_0$  beads which move on a given time step, then this gives a  $3N_0 \times 3N_0$  submatrix.

We use the Cholesky decomposition outlined by Ermak and McCammon<sup>24</sup> to get the lower triangular matrix  $\mathbf{B}$  such

TABLE I. An example of the model running on multiple time steps in two regions, where region 1 has twice finer resolution than region 2, so that  $2s_1 = s_2$ , which gives  $8\Delta t_1 = \Delta t_2$ . We run a time step using Eq. (18) for each bead in region 1 and region 2. The force terms  $\tilde{\mathbf{F}}_m(i\Delta t)$ , where bead  $m$  is in region 1, is summed over the small timesteps to give  $\tilde{\mathbf{F}}_{mn}(i\Delta t)$  on the larger timesteps. We use the same concept to find noise terms  $\tilde{\mathbf{X}}_{mn}(i\Delta t)$ .

	0	$\Delta t_1$	$2\Delta t_1$	$3\Delta t_1$	$4\Delta t_1$	$5\Delta t_1$	$6\Delta t_1$	$7\Delta t_1$	$8\Delta t_1$
$s_1$	•	•	•	•	•	•	•	•	•
$s_2$	○								○

that  $\mathbf{H} = \mathbf{B}\mathbf{B}^T$  with elements given by, for  $n = 1, 2, \dots, 3N_0$ ,

$$B_{nn} = \left( H_{nn} - \sum_{k=1}^{n-1} B_{nk}^2 \right)^{1/2},$$

$$B_{mn} = \frac{\left( H_{mn} - \sum_{k=1}^n B_{mk} B_{nk} \right)}{B_{mm}}$$

to give noise terms  $\tilde{\rho}_n$  with the calculation

$$\tilde{\rho}_n(i\Delta t) = \sum_{m=1}^n B_{nm} \tilde{X}_{mn}(i\Delta t),$$

which are then reordered and formatted to give  $\tilde{\rho}_n$  in a  $N_0 \times 3$  matrix. The random terms  $\tilde{X}_{mn}$  now include a “memory” similar to the tension terms so that

$$\tilde{X}_{mn}(i\Delta t) = \begin{cases} X_m(i\Delta t), & \text{if } s_{\alpha_n} < s_{\alpha_m}, \\ \sum_{p=0}^{(s_{\alpha_n}/s_{\alpha_m})^3 - 1} X_m((t-p)\Delta t), & \text{otherwise,} \end{cases}$$

for the terms  $X_m(t)$  drawn from a Gaussian normal distribution such that  $\langle X_m(t) \rangle = 0$  and  $\langle X_m(t_1) X_n(t_2) \rangle = 2k_B T \delta_{mn} \Delta t \alpha_n \delta(t_1 - t_2)$ .

## V. SIMULATIONS

We compare the full BD modeling with the dynamics using the pre-averaged tensor  $\langle \mathbf{H}_{mn} \rangle_{\text{eq}}$  from Eq. (12) in place of  $\mathbf{H}_{mn}$  in the Ermak-McCammon algorithm given above. Similar to previous papers simulating bead-spring models,<sup>33</sup> we choose to simulate with unit parameters, which in our case has  $k_B T = 1$  and  $\eta = 1$ . We shall also hold the rms end-to-end distance constant with  $\mu = 1$ , which we shall maintain by varying the statistical segment length  $b$  as a function of the bead number  $N$  as appropriate given the scalings explained in Sec. III B. To ensure numerical stability of simulations, we found  $\Delta t = 10^{-2} b^3 \eta / k_B T$  to be a good value to use.

In order to study the translational diffusion coefficient in simulations, we need to extend its definition for the simulations of the multi-resolution model. We define the mass of the polymer  $\Omega$  as

$$\Omega = \sum_{n=1}^N \sigma_n^2,$$

where  $\sigma_n$  is the radius of the  $n$ th bead,  $n = 1, 2, \dots, N$ . Using scalings (17), we observe that  $\Omega$  is invariant to our choice of resolutions in the multi-resolution scheme. This allows us to define the centre of mass of a polymer  $\mathbf{r}_G$  at time  $t$  as

$$\mathbf{r}_G(t) = \frac{\sum_{n=1}^N \mathbf{r}_n(t) \sigma_n^2}{\Omega},$$

where  $\mathbf{r}_n(t)$  is the position of the  $n$ th bead at time  $t$ . With this, we retain the definition of the translational diffusion coefficient as

$$D_G = \lim_{t \rightarrow \infty} \frac{1}{6t} \langle (\mathbf{r}_G(t) - \mathbf{r}_G(0))^2 \rangle. \quad (19)$$

Note that for the single-scale simulation this reduces to the standard definition for the translational diffusion coefficient.

In this section, we compare the translational diffusion coefficient approximations given in the form of an inverse matrix in Eq. (15) as well as the long-chain limit approximation in Eq. (16) to BD simulations for both the full mobility matrix as well as the pre-averaged approximation, as well as the rms end-to-end distance, which has an expected value 1 in all simulations by design. We run the BD simulations using both a pre-averaged and a non-pre-averaged (NPA) mobility tensor for a total of  $10^4$  time steps (in the case of multi-resolution simulations, this refers to time steps associated with the higher resolution beads), where each result is given as an average over 500 runs and contrast this to the diffusion approximations.

In the results Tables II and III, we include 95% confidence intervals for the translational diffusion coefficient and the rms

TABLE II. Results for diffusion and the rms end-to-end distance in single-scale simulations. The subscript MF represents the matrix formulation, PA is for pre-averaged, and NPA is for non-pre-averaged. The 95% confidence intervals for  $\mu_{\text{PA}}$  and  $\mu_{\text{NPA}}$  are given by  $CI_{\mu_{\text{PA}}}$  and  $CI_{\mu_{\text{NPA}}}$ , respectively.

$N$	$D_{\text{MF}}$	$D_{\text{PA}}$	$\mu_{\text{PA}}$	$CI_{\mu_{\text{NPA}}}$	$D_{\text{NPA}}$	$\mu_{\text{NPA}}$	$CI_{\mu_{\text{NPA}}}$
5	0.178	$0.187 \pm 0.013$	0.99	[0.96, 1.01]	$0.180 \pm 0.013$	1.00	[0.96, 1.03]
10	0.184	$0.195 \pm 0.015$	0.99	[0.96, 1.03]	$0.185 \pm 0.014$	1.00	[0.97, 1.04]
30	0.189	$0.192 \pm 0.013$	1.00	[0.97, 1.04]	$0.186 \pm 0.013$	1.00	[0.96, 1.03]
50	0.191	$0.202 \pm 0.014$	1.01	[0.98, 1.05]	$0.180 \pm 0.013$	1.01	[0.97, 1.04]
100	0.191	$0.188 \pm 0.013$	1.01	[0.98, 1.05]	$0.174 \pm 0.012$	1.01	[0.98, 1.05]
200	0.192	$0.184 \pm 0.013$	0.99	[0.96, 1.03]	$0.193 \pm 0.014$	1.00	[0.96, 1.04]

TABLE III. Results for diffusion and the rms end-to-end distance in multi-resolution simulations, which have the middle 25% of the polymer in high resolution. Subscripts are the same as in Table II. Simulations run for  $10^4$  time steps for beads at the highest resolution.

$N$	$D_{\text{MF}}$	$D_{\text{PA}}$	$\mu_{\text{PA}}$	$CI_{\mu_{\text{NPA}}}$	$D_{\text{NPA}}$	$\mu_{\text{NPA}}$	$CI_{\mu_{\text{NPA}}}$
32	0.191	$0.183 \pm 0.013$	0.99	[0.95, 1.02]	$0.189 \pm 0.013$	1.02	[0.98, 1.05]
64	0.191	$0.195 \pm 0.013$	0.99	[0.95, 1.02]	$0.186 \pm 0.014$	0.99	[0.96, 1.03]
128	0.192	$0.185 \pm 0.014$	1.00	[0.96, 1.04]	$0.192 \pm 0.013$	1.00	[0.97, 1.04]
256	0.192	$0.186 \pm 0.013$	1.00	[0.96, 1.03]	$0.184 \pm 0.014$	0.98	[0.94, 1.01]

end-to-end distances. For the end-to-end distance, we calculate the 95% confidence interval for  $\langle \mathbf{R}^2 \rangle$  and take the square root for both lower and upper bounds to give a range (note that this is not symmetric about the rms value).

We consider three illustrative examples. The first one is a single-scale system so that  $M = 1$  and  $s_1 = 1$ . We use the single-scale system to show the accuracy of our analytic results, which are later used for comparison to multi-resolution simulations. Our results are presented in Fig. 1 and Table II. As we can see in the table, the matrix formulation  $D_{MF}$  is covered within the 95% confidence interval, all except one of the pre-averaged and non-pre-averaged values of  $N$ . The analytic value of  $\mu = 1$  fits in the confidence interval for all simulations.

The next system to consider is the one in which the middle 25% of the polymer is in high resolution, while the remainder is coarse grained by a factor of 2. Therefore we define  $M = 3$  with  $s_1 = 2$ ,  $s_2 = 1$ ,  $s_3 = 2$  and  $\tilde{N}_1 = 3N/8$ ,  $\tilde{N}_2 = N/4$ ,  $\tilde{N}_3 = 3N/8$ . The diffusion and the rms end-to-end distance of this polymer are given in Table III. The matrix formulation for the diffusion  $D_{MF}$  is contained in the confidence intervals for all values of  $N$ , and the value of  $\mu = 1$  is contained in the confidence interval for all values of  $N$ . The convergence of matrix formulation to the long-chain limit is shown in Fig. 1.

The final system considered had an 8-times resolution increase in the middle 10% of the polymer. This uses  $M = 3$  with  $s_1 = 8$ ,  $s_2 = 1$ ,  $s_3 = 8$  and  $\tilde{N}_1 = 9N/20$ ,  $\tilde{N}_2 = N/10$ ,  $\tilde{N}_3 = 9N/20$ . We perform the simulation for  $N = 1280$ , from which we can report  $D = 0.189$ ,  $\mu = 1.04$  for the pre-averaged case and  $D = 0.180$ ,  $\mu = 1.01$  where we do not use pre-averaging. The matrix formulation for the translational diffusion coefficient gives a value  $D_{MF} = 0.190$ . The end-to-end distance in the pre-averaged case narrowly falls out of the 95% confidence interval, but the other three statistics lie within this range.

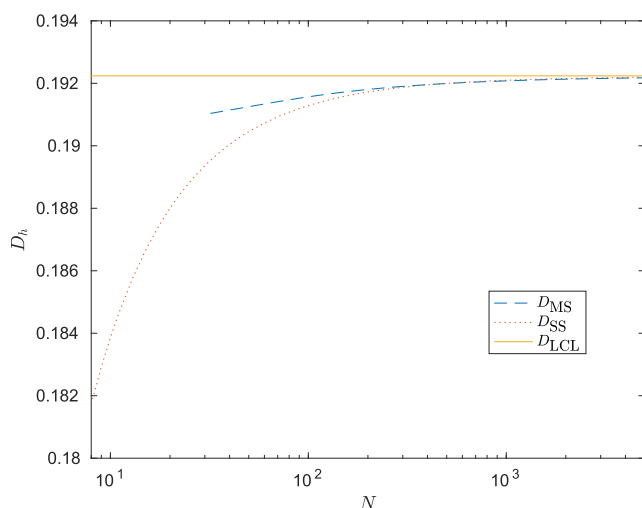


FIG. 1. The difference between the matrix formulation for the diffusion coefficient (15) and the long-chain limit (16) as  $N$  gets large, for both the single-scale system (red dotted line) and the multiscale simulation, which has the middle 25% of the polymer in high resolution (blue dashed line). Parameters are given in Sec. V. Note that the multi-scale system needs  $N \geq 32$  by construction for the coarse-grained particles to be placed.

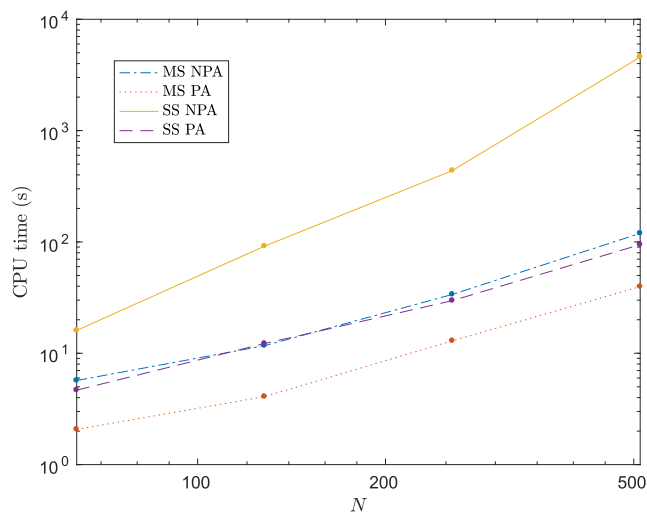


FIG. 2. The CPU times to simulate identical systems using four different algorithms: the multi-scale model using pre-averaging (red dotted line), the single-scale model with pre-averaging (purple dashed line), the multi-scale model without pre-averaging (blue dot-dashed line), and the single-scale model without pre-averaging (yellow solid line).

As can be seen from the simulations, there is good agreement both between the pre-averaged and non pre-averaged tensors and between the diffusion approximations and the results from the simulations. In total, out of 44 observations, we had two falling outside of the 95% confidence interval. The overall goal of doing this coarse graining is to improve the speed of simulations. In Fig. 2, we compared the timings between the single-scale and multi-scale models for identical parameters, as were used to produce Table III. There is a pronounced difference between the multi-scale model and single-scale model without pre-averaging, most of which comes from having to use the Cholesky decomposition on smaller matrices, while the smaller difference in the model with pre-averaging comes from updating fewer beads in each time step.

There are different situations in which it would be useful to use the pre-averaging approach for simulations and other situations where it would be better to use the full multiscale method. It has been long known that pre-averaging the mobility matrix results in a miscalculation in intrinsic viscosity and other rheological properties due to a nonvanishing second normal stress difference.<sup>14,34</sup> Therefore, for simulations where these properties of the polymer are important and computational efficiency is less of an issue, then using the full hydrodynamic interaction tensor would be more appropriate. However, if speed is more important, then there can be significant gains from taking the pre-averaged approximation. More study would be needed on the effect of multi-resolution modeling on the errors introduced by taking the pre-averaging approach.

## VI. DISCUSSION

In this paper, we have extended the bead-spring model for a polymer including hydrodynamic interactions to a multi-resolution model in order to gain computational efficiency



for BD modeling. By considering a multi-resolution Gaussian chain model, we have utilised the Boltzmann distribution in order to form a diffusive displacement equation for the multi-resolution model. From this, we used a similar approach to that of Öttinger<sup>15</sup> in order to derive an integral equation for the diffusion of the polymer using the pre-averaging approximation, which was then manipulated to find a closed form equation for the diffusion in the long-chain limit. This gave scaling laws for key parameters of the polymer at different scales. The developed multi-resolution approach keeps the rms end-to-end distance and the diffusion of the polymer invariant to the choices of how we split the polymer up into different resolutions. These scaling laws have then been supported by illustrative simulations, which used an adapted version of the Ermak-McCammon algorithm.<sup>24</sup>

The intention of this paper is to act as a stepping stone toward a more full multi-resolution approach to be applied to BD models for polymers, incorporating more detailed and accurate models for a polymer as well as faster algorithms into which a large amount of research has been done over the past 30 years. We have used the Hookean potential between beads due to its mathematical tractability, though a numerical approach could be used to extend this to other spring potentials. We chose the numerical method as it was one of the first presented; it is also expected that this could be extended to more modern algorithms.

The use of a Hookean potential between beads allows us to describe the inter-bead distances in terms of a Gaussian, which makes it much mathematically easier to analyze. This can introduce unrealistic features, for example, the linear force as the length of the spring gets very long, which can be addressed by extending the model to the finitely extensible non-linear elastic polymer model (often known as the FENE spring).<sup>29</sup> There are also more elaborate potentials introduced for specific modeling of DNA on mesoscopic scales in the literature,<sup>3,35,36</sup> for example, the 3SPN model of DNA,<sup>37</sup> which uses three sites per nucleotide and can describe the more complicated dynamics found on these scales. A further extension of this work could be to extend these models to a corresponding multi-resolution approach, similar to the multi-resolved polymer chain of Di Pasquale-Carbone<sup>38</sup> or even to introduce a hybrid model where different models are combined between regions. Due to the intractability of these more advanced potentials, in order to maintain macroscale quantities, a numerical approach would be necessary.

We believe that this approach could also be extended to include excluded volume interactions to allow for the study of a good solvent, building on existing analytical work<sup>7,39-41</sup> to provide scaling laws and extending the soft-core Gaussian approach<sup>28,42,43</sup> for Brownian dynamics simulations. It is imagined that this would involve a computer-assisted parameter search for each region of the polymer to investigate how properties of interest scale. Computational explorations of multi-region polymer models would then be used to select an appropriate mechanism to glue the different regions of the polymer together in one dynamical multi-resolution simulation.

There have also been many developments in the algorithms which are used to study polymers with hydrodynamic interactions.<sup>20-23</sup> Many of these algorithms operate with approximations allowing them to run in  $\mathcal{O}(N)$  time<sup>44,45</sup> which would decrease computational gains from the multi-resolution concept, but as an approach, the multi-resolution bead-spring model would still be important for reducing computation time, particularly in situations where there are large differences in the temporal and spatial scales of the system. It is hoped that these could, in theory, be extended to multi-resolution modeling using a similar approach to the one taken in this paper.

## ACKNOWLEDGMENTS

This work was supported by funding from the Engineering and Physical Sciences Research Council (EPSRC) (Grant No. EP/G03706X/1). Radek Erban would also like to thank the Royal Society for a University Research Fellowship.

## APPENDIX: DERIVATION OF THE LONG-CHAIN LIMIT

In this section, we simplify Eq. (15) in the long-chain limit,  $N \rightarrow \infty$ , which is taken in such a way that the fraction of springs in each region,  $N_\alpha/(N-1)$ , remains a constant; i.e., if  $(N-1)$  doubles in size, then each individual region also doubles in size.

We assume that the  $\alpha$ th region contains  $N_\alpha$  springs, with statistical segment length  $b_\alpha$ ,  $\alpha = 1, 2, \dots, M$ . Summing over all regions, we have

$$\sum_{\alpha=1}^M N_\alpha = N - 1.$$

Equation (12) defines a function of two integer variables  $m$  and  $n$ . We will map the discrete function  $\hat{H}_{mn}$  into a continuous function  $H(x, y)$  by generalizing the approach of Öttinger<sup>28</sup> and Fixman.<sup>16</sup> Assuming that bead  $m$  lies in region  $\alpha$ , its continuous approximation in interval  $[-1, 1]$  will be defined by

$$\frac{2b_\alpha^2}{\mu^2} m - 1 + \frac{2}{\mu^2} \sum_{\gamma=1}^{\alpha-1} N_\gamma (b_\gamma^2 - b_\alpha^2) \rightarrow x, \quad (\text{A1})$$

where  $\mu^2 = \sum_{\gamma=1}^M N_\gamma b_\gamma^2$ . The continuous analog of a summation of arbitrary function  $f_n$  over all beads will then be a weighted integral

$$\sum_{n=1}^N f_n \rightarrow \int_{-1}^1 f(x) b(x) dx, \quad (\text{A2})$$

where we define  $b(x)$  as a piecewise constant function given by  $b(x) = \mu^2 b_\alpha^{-2}/2$  in the interval

$$x \in \left( \frac{2}{\mu^2} \sum_{\gamma=1}^{\alpha-1} N_\gamma b_\gamma^2 - 1, \frac{2}{\mu^2} \sum_{\gamma=1}^{\alpha} N_\gamma b_\gamma^2 - 1 \right).$$

In addition to (A1), we also write for bead  $n$  in region  $\beta$

$$\frac{2b_\beta^2}{\mu^2} n - 1 + \frac{2}{\mu^2} \sum_{\gamma=1}^{\beta-1} N_\gamma (b_\gamma^2 - b_\beta^2) \rightarrow y.$$

This leads to a transformation  $(m, n) \rightarrow (x, y)$ , which gives the continuous approximation of  $\hat{H}_{mn}$  in  $[-1, 1] \times [-1, 1]$  as

$$H(x, y) = \sqrt{\frac{2}{\mu^2}} \frac{1}{\eta \pi \sqrt{6\pi|x-y|}}. \quad (\text{A3})$$

The definition of the inverse of the matrix  $\hat{H}_{mn}$  (given as  $\sum_{k=1}^N \hat{H}_{mk} \hat{H}_{kn}^{-1} = \delta_{mn}$ ) is rewritten in continuous variables as

$$\int_{-1}^1 H(x, z) H^{-1}(z, y) b(z) dz = \frac{\delta(x-y)}{b(x)}.$$

Multiplying both sides by  $b(y)$ , integrating over  $y$ , and using (A3), we obtain

$$\int_{-1}^1 \frac{\phi(z)}{\sqrt{|x-z|}} dz = \eta \mu \pi \sqrt{3\pi}, \quad (\text{A4})$$

where

$$\phi(z) = \int_{-1}^1 b(y) b(z) H^{-1}(z, y) dy.$$

Using the method of Auer and Gardner,<sup>16,46</sup> we solve Eq. (A4) for  $\phi(z)$  to obtain

$$\phi(z) = \frac{\eta \mu \sqrt{3\pi}}{\sqrt{2} (1-z^2)^{1/4}}.$$

To return to the quantity of interest,  $\sum \sum \hat{H}_{nm}^{-1}$ , we apply the mapping from Eq. (A2) to give

$$\begin{aligned} \sum_{n=1}^N \sum_{m=1}^N \hat{H}_{nm}^{-1} &= \int_{-1}^1 \int_{-1}^1 b(x) b(y) H^{-1}(x, y) dy dx \\ &= \int_{-1}^1 \phi(x) dx = \frac{\eta \mu 4\pi^2 \sqrt{3}}{\Gamma^2(1/4)}, \end{aligned}$$

where  $\Gamma$  is the gamma function. Substituting in (15), we obtain the diffusion constant in the long-chain limit given by Eq. (16).

<sup>1</sup>Z. Zhang and D. Thirumalai, *Structure* **20**, 628 (2012).

<sup>2</sup>R. M. Jendrejack, J. J. de Pablo, and M. D. Graham, *J. Chem. Phys.* **116**, 7752 (2002).

<sup>3</sup>C. M. Schroeder, E. S. Shaqfeh, and S. Chu, *Macromolecules* **37**, 9242 (2004).

<sup>4</sup>S. R. Quake, H. Babcock, and S. Chu, *Nature* **388**, 151 (1997).

<sup>5</sup>S. Amelar, C. Eastman, R. Morris, M. Smeltzly, T. Lodge, and E. Von Meerwall, *Macromolecules* **24**, 3505 (1991).

<sup>6</sup>D. W. Hair and E. J. Amis, *Macromolecules* **22**, 4528 (1989).

<sup>7</sup>M. Doi and S. F. Edwards, *The Theory of Polymer Dynamics* (Oxford University Press, 1988).

<sup>8</sup>R. Erban, *Proc. R. Soc. A* **470**, 20140036 (2014).

<sup>9</sup>R. Erban, *Proc. R. Soc. A* **472**, 20150556 (2016).

<sup>10</sup>N. Korolev, L. Nordenskiöld, and A. P. Lyubartsev, *Adv. Colloid Interface Sci.* **232**, 36 (2016).

<sup>11</sup>J. Zavadlav, R. Podgornik, and M. Praprotnik, *J. Chem. Theory Comput.* **11**, 5035 (2015).

<sup>12</sup>E. Rolls, Y. Togashi, and R. Erban, *Multiscale Model. Simul.* **15**, 1672 (2017).

<sup>13</sup>J. G. Kirkwood and J. Riseman, *J. Chem. Phys.* **16**, 565 (1948).

<sup>14</sup>B. H. Zimm, *J. Chem. Phys.* **24**, 269 (1956).

<sup>15</sup>H. C. Öttinger, *J. Chem. Phys.* **87**, 3156 (1987).

<sup>16</sup>M. Fixman, *Macromolecules* **14**, 1710 (1981).

<sup>17</sup>J. Rotne and S. Prager, *J. Chem. Phys.* **50**, 4831 (1969).

<sup>18</sup>H. Yamakawa, *J. Chem. Phys.* **53**, 436 (1970).

<sup>19</sup>P. Zuk, E. Wajnryb, K. Mizerski, and P. Szymczak, *J. Fluid Mech.* **741**, R5 (2014).

<sup>20</sup>L. Miao, C. D. Young, and C. E. Sing, *J. Chem. Phys.* **147**, 024904 (2017).

<sup>21</sup>M. Fixman, *Macromolecules* **19**, 1204 (1986).

<sup>22</sup>T. Ando, E. Chow, Y. Saad, and J. Skolnick, *J. Chem. Phys.* **137**, 064106 (2012).

<sup>23</sup>T. Geyer and U. Winter, *J. Chem. Phys.* **130**, 114905 (2009).

<sup>24</sup>D. L. Ermak and J. A. McCammon, *J. Chem. Phys.* **69**, 1352 (1978).

<sup>25</sup>H. Rezvantab and R. G. Larson, *Macromolecules* **51**, 2125 (2018).

<sup>26</sup>H. Rezvantab, G. Zhu, and R. G. Larson, *Soft Matter* **12**, 5883 (2016).

<sup>27</sup>P. T. Underhill and P. S. Doyle, *J. Non-Newtonian Fluid Mech.* **122**, 3 (2004).

<sup>28</sup>H. C. Öttinger, *Stochastic Processes in Polymeric Fluids: Tools and Examples for Developing Simulation Algorithms* (Springer Science & Business Media, 1996).

<sup>29</sup>R. B. Bird, R. C. Armstrong, O. Hassager, and C. Curtiss, *Dynamics of Polymeric Liquids-Volume 2: Kinetic Theory* (Wiley, 1987).

<sup>30</sup>R. G. Larson, *J. Rheol.* **49**, 1 (2005).

<sup>31</sup>H. C. Öttinger, *J. Chem. Phys.* **86**, 3731 (1987).

<sup>32</sup>A. Saadat and B. Khomami, *J. Chem. Phys.* **140**, 184903 (2014).

<sup>33</sup>B. Liu and B. Dünweg, *J. Chem. Phys.* **118**, 8061 (2003).

<sup>34</sup>J. R. Prakash and H. C. Öttinger, *J. Non-Newtonian Fluid Mech.* **71**, 245 (1997).

<sup>35</sup>Y. Goldtzyk, Z. Zhang, and D. Thirumalai, *J. Phys. Chem. B* **120**, 2071 (2016).

<sup>36</sup>A. Rosa and R. Everaers, *PLoS Comput. Biol.* **4**, e1000153 (2008).

<sup>37</sup>T. A. Knotts IV, N. Rathore, D. C. Schwartz, and J. J. de Pablo, *J. Chem. Phys.* **126**, 02B611 (2007).

<sup>38</sup>N. Di Pasquale and P. Carbone, *J. Chem. Phys.* **146**, 084905 (2017).

<sup>39</sup>K. F. Freed, *Renormalization Group Theory of Macromolecules* (Wiley, 1987).

<sup>40</sup>P. J. Flory, *J. Chem. Phys.* **17**, 303 (1949).

<sup>41</sup>H. C. Öttinger, *Phys. Rev. A* **40**, 2664 (1989).

<sup>42</sup>K. S. Kumar and J. R. Prakash, *Macromolecules* **36**, 7842 (2003).

<sup>43</sup>S. Pan, D. Ahirwal, D. A. Nguyen, T. Shridhar, P. Sunthar, and J. R. Prakash, *Macromolecules* **47**, 7548 (2014).

<sup>44</sup>J. P. Hernández-Ortiz, J. J. de Pablo, and M. D. Graham, *Phys. Rev. Lett.* **98**, 140602 (2007).

<sup>45</sup>B. Dünweg and A. J. Ladd, *Advanced Computer Simulation Approaches for Soft Matter Sciences III* (Springer, 2009), pp. 89–166.

<sup>46</sup>P. L. Auer and C. S. Gardner, *J. Chem. Phys.* **23**, 1545 (1955).